The Yeast Gene, *MDM20,* Is Necessary for Mitochondrial Inheritance and Organization of the Actin Cytoskeleton

Greg J. Hermann, Edward J. King, and Janet M. Shaw

Department of Biology, University of Utah, Salt Lake City, Utah 84112

Abstract. In *Saccharomyces cerevisiae*, the growing bud inherits a portion of the mitochondrial network from the mother cell soon after it emerges. Although this polarized transport of mitochondria is thought to require functions of the cytoskeleton, there are conflicting reports concerning the nature of the cytoskeletal element involved. Here we report the isolation of a yeast mutant, *mdm20*, in which both mitochondrial inheritance and actin cables (bundles of actin filaments) are disrupted. The *MDM20* gene encodes a 93-kD polypeptide with no homology to other characterized proteins. Extra copies of *TPM1*, a gene encoding the actin filament–binding protein tropomyosin, suppress mitochondrial inheritance defects and partially restore actin cables in *mdm20Δ* cells. Synthetic lethality is also observed between *mdm20* and *tpm1* mutant strains. Overexpression of a second yeast tropomyosin, Tpm2p, rescues mutant phenotypes in the *mdm20* strain to a lesser extent. Together, these results provide compelling evidence that mitochondrial inheritance in yeast is an actin-mediated process. *MDM20* and *TPM1* also exhibit the same pattern of genetic interactions; mutations in *MDM20* are synthetically lethal with mutations in *BEM2* and *MYO2* but not *SAC6.* Although *MDM20* and *TPM1* are both required for the formation and/or stabilization of actin cables, mutations in these genes disrupt mitochondrial inheritance and nuclear segregation to different extents. Thus, Mdm20p and Tpm1p may act in vivo to establish molecular and functional heterogeneity of the actin cytoskeleton.

MITOCHONDRIA are essential organelles whose morphology, copy number, and distribution can vary dramatically in different eukaryotic cell types (Bereiter-Hahn, 1990; Yaffe, 1991; Thorsness, 1992; Bereiter-Hahn and Voth, 1994; Warren and Wickner, 1996). Like all organelles that cannot be synthesized de novo, the mitochondrial compartment must grow, divide, and be delivered to newly formed daughter cells during division. While substantial progress has been made in identifying the molecular components that mediate mitochondrial biogenesis (Hannavy et al., 1993; Schwarz and Neupert, 1994; Kubrich et al., 1995; Ryan and Jensen, 1995; Lill and Neupert, 1996), a detailed picture of the mechanisms that control mitochondrial morphology, distribution, and motility throughout the cell cycle has not yet emerged.

In the budding yeast *Saccharomyces cerevisiae*, respiring mitochondria form an elaborate network of tubular membranes located near the cell periphery (Hoffman and Avers, 1973). Very early in the cell cycle (early S phase), a portion of this mitochondrial network is transported from the mother cell into the growing bud (Fig. 1) (Stevens, 1981). Recent genetic studies have identified a few proteins that control mitochondrial morphology and distribution in cells and mitochondrial transmission during cell division. These include Mdm10p and Mmm1p, two proteins of the outer mitochondrial membrane required for the maintenance of normal organelle morphology (Sogo and Yaffe, 1994, *mdm* [mitochondrial distribution and morphology]; Burgess et al., 1994, *mmm* [maintenance of mitochondrial morphology]; Mdm2p/Ole1p, a fatty acid desaturase that may regulate the level of unsaturated fatty acids in the mitochondrial membrane (Stukey et al., 1989, 1990; Stewart and Yaffe, 1991, *ole* [oleic acid requiring]); and Mdm1p, a protein with characteristics of the mammalian intermediate filament–like proteins keratin and vimentin (McConnell and Yaffe, 1992, 1993). In addition, there are several proteins that are required for the normal maintenance or segregation of mitochondrial DNA. Mgm1p is a member of the dynamin family of GTP binding proteins (Jones and Fangman, 1992; Guan et al., 1993; Backer, 1995; *mgm* [mitochondrial genome maintenance]); *ILV5* encodes a protein that plays an as yet unidentified role in mitochondrial genome maintenance (Zelenaya-Troitskaya et al., 1995; *ilv* [isoleucine-plus-valine requiring]); and Abf2p is an HMG1-like DNA binding protein (Diffley and Stillman, 1991, 1992; *abf* [ARS binding factor]). Studies are in progress in a number of laboratories to determine how the activities of these proteins control the behavior of the mi-

Please address all correspondence to Janet M. Shaw, Department of Biology, University of Utah, Salt Lake City, UT 84112. Tel.: (801) 585-6205. Fax: (801) 581-4668.

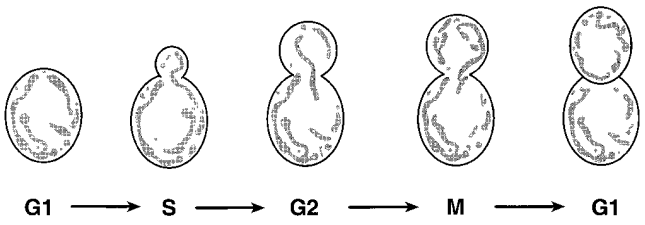

Figure 1. Mitochondrial inheritance during mitotic cell division. Mitochondria are localized near the cortex of unbudded and budding cells. Early in the cell cycle (S phase) a portion of the maternal mitochondrial network extends into the developing bud. As the bud grows (S phase to G2 phase), mitochondria continue to accumulate in the daughter cell. At cytokinesis (M phase/G1 phase boundary), the mitochondrial content of the daughter cell is often greater than that of the mother cell.

tochondrial compartment and the replication and segregation of the mitochondrial genome.

Most forms of organelle motility are directed by cytoskeletal structures and their associated motor proteins. Mitochondria have been reported to colocalize with actin filaments (Drubin et al., 1993), microtubules (Heggeness et al., 1978; Ball and Singer, 1982; Summerhayes et al., 1983), and intermediate filaments (Mose-Larsen et al., 1982; Summerhayes et al., 1983; Stromer and Bendayan, 1990) in different cell types, and recent studies indicate that mitochondria can be transported in a polarized fashion using both microtubule- (Nangaku et al., 1994; Morris and Hollenbeck, 1995; Hollenbeck, 1996) and actin-based (Kuznetsov et al., 1992; Morris and Hollenbeck, 1995; Simon et al., 1995; Hollenbeck, 1996) motors. In yeast, two different cytoskeletal elements, Mdm1p and actin, have been proposed to direct the transfer of mitochondria into yeast buds. Mdm1p shares structural features with mammalian intermediate filament proteins and will form 10-nm filaments in vitro (McConnell and Yaffe, 1992, 1993). Mutations in *MDM1* cause defects in mitochondrial morphology and also in both mitochondrial and nuclear inheritance, suggesting that this protein is important for organelle positioning and/or segregation.

Recent studies have also established a role for the yeast actin cytoskeleton in mitochondrial distribution and inheritance. Yeast cells contain a single, essential, conventional actin gene (*ACT1*) (Shortle et al., 1982; Welch et al., 1994). In vivo, actin is organized into two different types of structures: (*a*) cortical actin patches (invaginations of the plasma membrane associated with F-actin) and (*b*) actin cables (bundles of F-actin; Adams and Pringle, 1984; Mulholland et al., 1994). In mitotically dividing cells, cortical actin patches cluster in the growing bud, and actin cables aligned along the mother-bud axis are well positioned to deliver mitochondria to the daughter cell (Kilmartin and Adams, 1984). Mitochondria have been shown to colocalize with actin cables in yeast, and some mutations in actin result in abnormal mitochondrial morphology, distribution, and motility (Drubin et al., 1993; Lazzarino et al., 1994; Simon et al., 1995). In addition, recent studies established that isolated yeast mitochondria bind reversibly to phalloidin-stabilized actin filaments in vitro (Lazzarino et al., 1994). These mitochondria were shown in a related assay to contain a myosin-like actin-dependent motor activity on their surface (Simon et al., 1995). Based on these results, it has been suggested that yeast mitochondria are transported from the mother cell into the emerging bud using actin filaments as "tracks" and a myosin-like motor activity on the surface of the organelle.

To learn more about molecules that control mitochondrial inheritance, we screened a collection of yeast mutants for strains that failed to transport mitochondria into growing buds. In one of these mutants, *mdm20*, both mitochondrial inheritance and the organization of actin cables were disrupted. The *MDM20* gene encodes a novel 93-kD protein with no sequence similarities to proteins in the database. Extra copies of *TPM1*, a gene encoding the actin filament–binding protein tropomyosin, partially restored actin cables and suppressed mitochondrial inheritance defects in the *mdm20* strain. Furthermore, the combination of null mutations in *MDM20* and *TPM1* resulted in synthetic lethality. Overexpression of a second yeast tropomyosin, Tpm2p, also rescued actin organization defects and mitochondrial inheritance defects in *mdm20* cells, but to a lesser extent. Together, these results provide compelling evidence that mitochondrial inheritance in yeast is an actin-mediated process. Like *tpm1*, *mdm20* mutations are synthetically lethal with mutations in *BEM2* (Rho-GAP) and *MYO2* (type V myosin) but not *SAC6* (fimbrin). Thus, *TPM1* and *MDM20* exhibit the same pattern of genetic interactions. Despite the fact that mutations in *MDM20* and *TPM1* both result in the loss of observable actin cables in cells, we found that mitochondrial inheritance and nuclear segregation were disrupted to different extents in *mdm20* and *tpm1* mutant strains. Our results suggest that these two proteins act in vivo to establish molecular and functional heterogeneity of the actin cytoskeleton.

Materials and Methods

Strains, Media, and Genetic Techniques

Yeast strains used in this study are listed in Table I. Rich medium (yeast/peptone/dextrose [YPD] and yeast/peptone/glycerol [YPG]), synthetic medium (synthetic dextrose [SD] and synthetic galactose [SGal]), and media containing 5-fluoro-orotic acid (5-FOA)[1] were prepared as described by Sherman et al. (1986). Yeast mating, sporulation, tetrad dissection, complementation studies, and meiotic segregation analysis were performed using standard genetic techniques (Sherman et al., 1986). The lithium acetate method was used for all yeast transformations (Ito et al., 1983) and gene disruption experiments (Rothstein, 1991; Baudin et al., 1993). *Escherichia coli* strains DH5α and JM109 (Promega, Madison, WI) were used for bacterial manipulations of clones and plasmids. Molecular cloning techniques were performed as described by Maniatis et al. (1982).

Identification of mdm Mutants

The wild-type strain FY10 (Winston et al., 1995) was UV mutagenized (25% survival), and a collection of 4,000 temperature-sensitive yeast strains was generated. To identify mitochondrial distribution and morphology (*mdm*) mutants in this collection, individual strains were grown for 16 h at the permissive temperature (25°C) in 500 μl of YPD, diluted 1:10 into 500 μl fresh YPD, and shifted to the nonpermissive temperature (37°C) for 3 h. 100 μl of the culture was stained with a final concentration of 100 nM 3,3′

1. *Abbreviations used in this paper*: DAPI, 4′,6-diamidino-2-phenylindole; DIC, differential interference contrast; $DiOC_6$, 3,3′ dihexyloxacarbocyanine; 5-FOA, 5-fluoro-orotic acid; HA, hemagglutinin; SD, synthetic dextrose; SGal, synthetic galactose; Ura, uracil.

Table I. Yeast Strains Used in This Study

Name	Genotype*	Source
FY10	*MATα leu2Δ1 ura3-52*	F. Winston
FY22	*MATa his3Δ200 ura3-52*	F. Winston
GHY1	*MATα leu2Δ1 his3Δ200 ura3-52 mdm20-1*	This study
JSY707	*MATa his3Δ200 ura3-52 tpm1Δ::HIS3*	This study
JSY948	*MATa/α leu2Δ1/leu2Δ1 ura3-52/ura3-52*	This study
JSY999	*MATα leu2Δ1 his3Δ200 ura3-52*	This study
JSY1065	*MATα leu2Δ1 his3Δ200 ura3-52 mdm20Δ::LEU2*	This study
JSY1084	*MATa leu2Δ1 his3Δ200 ura3-52 tpm1Δ::HIS3*	This study
JSY1138	*MATa/α leu2Δ1/leu2Δ1 his3Δ200/his3Δ200 ura3-52/ura3-52 tpm1Δ::HIS3/+ mdm20Δ::LEU2/+*	This study
JSY1285	*MATα leu2Δ1 his3Δ200 ura3-52 tpm2Δ::HIS3*	This study
JSY1340	*MATa leu2Δ1 his3Δ200 ura3-52 mdm20Δ::LEU2*	This study
JSY1374	*MATa/α leu2Δ1/leu2Δ1 his3Δ200/his3Δ200 ura3-52/ura3-52 tpm2Δ::HIS3/+ mdm20Δ::LEU2/+*	This study
ABY1249	*MATa leu2-3,112 ura3-52 lys2-801 ade2-101 ade3 bem2-10*	A. Bretscher
IGY4	*MATα leu2-3,112 his3Δ200 ura3-52 lys2-801 ade2 sac6Δ::LEU2*	A. Adams
SLY63	*MATα leu2-3,112 ura3-52 trp1-Δ1 his6 myo2-66*	S. Brown

*All of the GHY and JSY strains used in this study are isogenic to FY10 (Winston et al., 1995).

dihexyloxacarbocyanine ($DiOC_6$) (Molecular Probes, Eugene, OR), and mitochondria were visualized by fluorescence microscopy. 18 *mdm* mutant strains were identified that produced large buds lacking $DiOC_6$-stained mitochondria. Standard genetic methods were used to show that the *mdm* phenotype in each strain was due to a single recessive mutation. In all but one case, the *mdm* phenotype was linked to the temperature-sensitive growth defect in three or more backcrosses to the wild-type parent. The exception was *mdm29*, which exhibited only a mitochondrial morphology defect. Complementation analysis was performed between the 18 *mdm* mutants identified in this screen and the existing *mdm* and *mmm* mutants generously provided by M. Yaffe (University of California, San Diego) (McConnell et al., 1990; Sogo and Yaffe, 1994) and R. Jensen (Johns Hopkins University, Baltimore, MD) (Burgess et al., 1994). One mutation was allelic to the previously identified *mdm2*/*ole1* gene (Stukey et al., 1989, 1990; Stewart and Yaffe, 1991). The remaining 17 *mdm* mutants define 10 new complementation groups designated *mdm20-mdm29.*

Cloning, Sequencing, and Disruption of MDM20 and Identification of TPM1 as an Unlinked Suppressor

An *mdm20-1* strain (GHY1) that had been backcrossed three times to the wild-type parent strains FY10 and FY22 was transformed with a yeast genomic library contained within the low copy plasmids YCp50 (Rose et al., 1987) (obtained from the American Type Culture Collection, Rockville, MD) and p366 (kindly provided by T. Formosa, University of Utah, Salt Lake City). 12,000 Ura^+ transformants containing the YCp50 library were tested for complementation of the temperature-sensitive growth defect in the *mdm20-1* strain. 14 colonies contained rescuing plasmids. Restriction digest and sequence analysis showed that these strains contained six different overlapping genomic inserts. The plasmid A6-2p, containing a 9-kb genomic insert, was selected for further analysis. A 1.6-kb BsaBI/KpnI fragment from A6-2p inserted into pRS416 (low copy CEN plasmid) or pRS426 (multicopy 2μ plasmid) (Stratagene, La Jolla, CA) digested with KpnI and SmaI was sufficient for complementation of the temperature-sensitive growth defect in *mdm20-1* cells. The sequence of a large genomic region containing this fragment was released as part of the Yeast Genome Sequencing Project (GenBank accession number X86470), and the 1.6-kb fragment was shown to contain only the *TPM1* gene. Integrative mapping (Rose and Broach, 1991) revealed that *mdm20* is not linked to *TPM1.* Thus, *TPM1* is an unlinked extra copy suppressor of the *mdm20* mutation.

The *MDM20* gene was isolated by transforming the *mdm20-1* strain GHY1 with the p366 genomic library. Of the 23,000 Leu^+ transformants screened, 24 contained plasmids that could rescue the temperature-sensitive growth defect in *mdm20-1* cells. Of these 24 plasmids, restriction digestion and Southern analysis revealed that seven contained *TPM1.* The remaining 17 plasmids contained four different genomic inserts that shared common overlapping restriction fragments. Plasmid A15-5p contained a 5.2-kb SphI fragment that, when cloned into YCp50, was sufficient to fully complement the *mdm20-1* mutation. The DNA carried by this plasmid was sequenced on both strands using an ABI373 automated sequencer at the University of Utah Health Sciences Sequencing Facility (supported by National Cancer Institute grant 5-P30CA42014). Deletion mapping and transposon mutagenesis (Sedgwick and Morgan, 1994) revealed that a 2,388-bp open reading frame was responsible for complementation. A Pfu polymerase (Stratagene) generated a PCR fragment containing the open reading frame, and 500 bp of 5′ and 3′ flanking sequence was subcloned into the EagI and SalI sites of pRS416 and pRS426. The two resulting plasmids complemented both the temperature-sensitive growth defects and mitochondrial inheritance defects in *mdm20-1* cells. The wild-type sequence of the *MDM20* gene inserted into both plasmids was verified by sequence analysis. Meiotic segregation analysis showed that the cloned open reading frame (*MDM20*) mapped to the *mdm20-1* mutation. The predicted Mdm20 protein sequence was compared with all available databases using the FASTA (Pearson and Lipman, 1988), BLAST (Altschul et al., 1990), and Prosite (Bairoch et al., 1995) programs. No significant homologies were detected. The putative coiled-coil domains in the Mdm20p were found using the COILS 2.1 program (Lupas et al., 1991). The *MDM20* GenBank accession number is U54799.

To generate the *mdm20* null mutation (*mdm20Δ*), a 1.9-kb *LEU2* PCR fragment was subcloned into pRS406-*MDM20* digested with HindIII and SpeI, replacing 2,219 bp (codon 12–751) of the *MDM20* open reading frame with *LEU2.* Digesting this plasmid with SalI and EagI released a 2.9-kb fragment containing the *LEU2* gene bordered by *MDM20*-flanking sequences that was used to transform the diploid yeast strain JSY948. The *mdm20Δ::LEU2* disruption was confirmed by Southern blotting of genomic DNA isolated from a Leu^+ transformant. Tetrad analysis of sporulated diploids confirmed that the *LEU2* marker cosegregated 2:2 with *mdm20* phenotypes (temperature sensitivity and defective mitochondrial inheritance) and that cells harboring the *mdm20Δ* mutation were viable at 25°C. To document the mitochondrial inheritance defect in the *mdm20Δ* strain, wild-type (JSY999) and isogenic *mdm20Δ* (JSY1065) cells were stained with $DiOC_6$ and examined microscopically as described below.

Suppression of the Temperature-sensitive and Organelle Inheritance Defects in mdm20Δ Cells

To examine the suppression of the *mdm20Δ* temperature-sensitive growth defect by *TPM1*, the wild-type (JSY999) or isogenic *mdm20Δ* (JSY1065) strains harboring pRS426, pRS426-*MDM20*, or pRS426-*TPM1* were grown to log phase at 25°C in SD minus uracil (SD − Ura) liquid medium. Equal numbers of cells were then serially diluted and spotted on SD − Ura solid media and grown at 37°C for 3 d. To examine the suppression of the *mdm20Δ* temperature-sensitive growth defect by *TPM2*, the wild-type (JSY999) or isogenic *mdm20Δ* (JSY1065) strains harboring pRS416, pRS416-*MDM20*, or *GAL1-TPM2* (pEH006; a generous gift from E. Harsay and A. Bretscher, Cornell University, Ithaca, NY) were grown to log phase at 25°C in SGal − Ura liquid medium. Equal numbers of cells were then serially diluted and spotted on SGal − Ura solid media and grown at 37°C for 3 d.

To determine the effects of extra copies of *TPM1* and *TPM2* on the mitochondrial and nuclear inheritance defects in *mdm20Δ* cells, the wild-type (JSY999) or *mdm20Δ* (JSY1065) strains harboring pRS416 or pRS426, pRS426-*TPM1*, or *GAL1-TPM2* were grown in SGal − Ura or SD − Ura liquid media for 16 h at 25°C, diluted, and grown in log phase at 25° or

37°C for 3 h. Mitochondrial inheritance was evaluated by $DiOC_6$ staining as described above. Nuclear segregation was analyzed by 4′,6-diamidino-2-phenylindole staining (DAPI) as described previously (Pringle et al., 1991). In each experiment, at least 400 cells were counted. *tpm1Δ* (JSY707) cells were examined for defects in mitochondrial and nuclear inheritance using the same protocol.

Characterization of Mdm20p-HA Expression

To monitor Mdm20p levels, the protein was tagged by the addition of three hemagglutinin (HA) epitopes at the amino and carboxy termini. A 3.1-kb SalI/HpaI fragment from pRS416-*MDM20* was inserted into p-ALTER-1 (Promega) digested with SalI and SmaI to create p-ALTER-1-*MDM20.* Site-directed mutagenesis (Altered Sites II; Promega) was used to insert NotI sites immediately downstream from the initiating Met or the carboxy-terminal Lys of *MDM20.* An NotI fragment from plasmid GTEP1 containing three tandem HA epitopes was inserted into the NotI sites at the 5′ or 3′ ends of *MDM20.* The correct orientation was verified by sequence analysis. *MDM20*-N-HA and *MDM20*-C-HA SalI/KpnI fragments were inserted into pRS416 and pRS426 digested with SalI and KpnI to create pRS416-*MDM20*-N-HA, pRS426-*MDM20*-N-HA, pRS416-*MDM20*-C-HA, and pRS426-*MDM20*-C-HA. All of the *MDM20*-HA constructs fully rescued the temperature-sensitive growth defect, the mitochondrial inheritance defect, and the loss of actin cables in *mdm20Δ* cells (JSY1065), indicating that the fusion proteins are functional.

To detect the Mdm20p–HA fusion proteins, 10^8 cells from log phase cultures were harvested and lysed using 0.2-mm glass beads in 500 μl of SDS-PAGE sample buffer. 25 μl of each lysate was loaded onto an 8% SDS-PAGE gel, and, after electrophoresis, the proteins were transferred to nitrocellulose. Western blot analysis was performed using standard protocols (Harlow and Lane, 1988). Mdm20p–HA fusion proteins were detected with polyclonal rabbit antibodies against HA (1:1,000) (BAbCO, Richmond, CA). Detection was carried out using the ECL kit (New England Nuclear, Boston, MA). The fusion proteins encoded by the *MDM20*-N-HA and *MDM20*-C-HA constructs have a predicted molecular mass of 97 kD but migrated with an apparent molecular mass of 90 kD on SDS-PAGE gels. Since the amino- and carboxy-terminal HA-tagged Mdm20p gave identical results, the aberrant size is likely not due to proteolysis, but instead may result from some structural feature or posttranslational modification of the fusion proteins. Comparison of Mdm20p–HA levels was performed using NIH Image 1.60 (National Institutes of Health, Bethesda, MD).

Synthetic Interactions Involving mdm20

The effects of combining *mdm20Δ* with *tpm1Δ* or *tpm2Δ* mutations were determined by constructing diploids heterozygous for *mdm20Δ* and *tpm1Δ* (JSY1138) or *mdm20Δ* and *tpm2Δ* (JSY1374). The *tpm1Δ* mutation was generated by transforming the wild-type strain FY22 with a PCR fragment containing 50 bp of *TPM1* flanking sequence interrupted by the *HIS3* gene using the technique described by Baudin et al. (1993). The disruption removes all but 42 bp of the 3′ *TPM1* coding region. The disruption in JSY707 was verified by Southern analysis. The *tpm2Δ* disruption was constructed in JSY999 using the *TPM2* disruption plasmid pBD103 (a gift from A. Bretscher) as described previously (Drees et al., 1995) to produce the *tpm2Δ::HIS3* strain JSY1285. The *tpm2Δ::HIS3* disruption was verified by Southern analysis. The heterozygous diploids JSY1138 and JSY1374 were sporulated, and tetrads were dissected. The *tpm1Δ::HIS3 mdm20Δ::LEU2* mutants germinated and gave rise to microcolonies containing 50–100 cells. In separate experiments, *tpm1Δ::HIS3 mdm20Δ::LEU2* double mutants were recovered when JSY1138 diploids containing the wild-type *MDM20* gene on a *URA3* plasmid were sporulated and dissected. The synthetic growth defect of *mdm20Δ tpm1Δ* double mutants was verified by showing that these cells were unable to lose the plasmid when grown on 5-FOA–containing medium. The JSY1374 diploid gave rise to viable *mdm20Δ::LEU2 tpm2Δ::HIS3* double mutants with no obvious synthetic growth defects. Crosses to test possible synthetic interactions between *mdm20Δ::LEU2* and *bem2-10* (Wang and Bretscher, 1995), *myo2-66* (Johnston et al., 1991), and *sac6Δ::LEU2* (Adams et al., 1991) were performed essentially as described above.

Analysis of the Actin Cytoskeleton in mdm20Δ and tpm1Δ Cells

To visualize F-actin, the wild-type (JSY999) or *mdm20Δ* (JSY1065) strains containing pRS426 were grown 16 h at 25°C in SD − Ura liquid medium. The cultures were then diluted (to 2×10^6 cells per ml) into fresh SD − Ura and grown at 25° or 37°C for 3 h. F-actin was detected with rhodamine-phalloidin (Molecular Probes) as described previously (Adams and Pringle, 1991). To determine the effects of overexpressing *TPM1* and *TPM2* on the actin cytoskeleton in *mdm20Δ* mutants, the *mdm20Δ* strain JSY1065 carrying pRS426-*TPM1* or *GAL1-TPM2* was grown in SD − Ura or SGal − Ura at 25° or 37°C as described above, and then stained with rhodamine-phalloidin. To analyze the effects of Mdm20p–HA overexpression on actin organization in *tpm1Δ* cells, the *tpm1Δ* strain JSY707 carrying pRS426, pRS426-*MDM20*, or pRS426-*MDM20*-C-HA was grown and stained as described above.

Microscopy

Cells were viewed on an Axioplan microscope using a ×100 Plan-neofluor (NA 1.3) objective (Carl Zeiss, Inc., Thornwood, NY) using an optivar setting of ×1.6, a 200-W mercury lamp, and the following excitation wavelengths: $DiOC_6$ (450–490 nm), DAPI (365 nm), and rhodamine (546 nm). Differential interference contrast (DIC) and fluorescence digital images were captured and assembled into figures as described previously (Roeder and Shaw, 1996). Images were printed on a Tektronix Phaser IIsdx dye-sublimation printer (Wilsonville, OR).

Results

mdm20 Mutants Exhibit Defects in Mitochondrial Inheritance

To identify yeast genes required for mitochondrial inheritance, we generated and screened a collection of temperature-sensitive mutants for strains that failed to transport mitochondria into growing buds. Individual strains grown at 25°C were shifted to 37°C for 3 h and stained with the lipophilic, fluorescent dye, $DiOC_6$, under conditions that preferentially label yeast mitochondria (Pringle et al., 1989; Shaw and Wickner, 1991; Koning et al., 1993). 18 of the 4,000 mutants examined exhibited defects in mitochondrial distribution and/or morphology. The mutations in these strains were recessive in heterozygous diploids

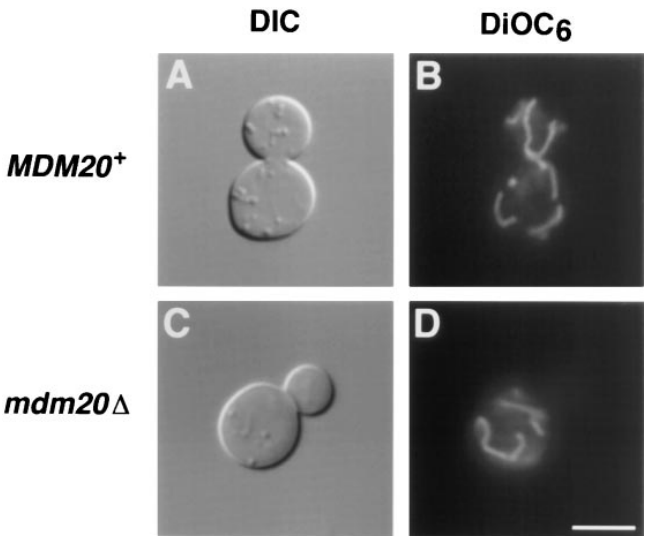

Figure 2. Cells lacking *MDM20* have normal mitochondrial morphology but do not segregate mitochondria into buds at 37°C. DIC images (*A* and *C*) and $DiOC_6$ mitochondrial staining (*B* and *D*) of *MDM20*$^+$ (JSY999) (*A* and *B*) and *mdm20Δ* (JSY1065) (*C* and *D*) cells grown at 37°C for 3 h. Bar, 5 μm.

Table II. Mitochondrial Inheritance in mdm20 and tpm1 Mutants

Genotype/(Plasmid)*	°C				
Wild type	25	48	52	0	0
Wild type	37	55	45	<1	0
mdm20Δ	25	37	49	14	<1
mdm20Δ	37	36	6	53	5
mdm20Δ + (pRS426-*TPM1*)	25	46	52	2	0
mdm20Δ + (pRS426-*TPM1*)	37	41	42	17	0
mdm20Δ + (*GAL1-TPM2*)‡	25	39	52	9	0
mdm20Δ + (*GAL1-TPM2*)	37	46	20	34	0
tpm1Δ	25	42	57	1	0
tpm1Δ	37	45	50	4	1

Mitochondrial inheritance scored in log-phase cells grown at 25° or 37°C for 3 h. The cartoons depict classes scored and include unbudded/small-budded, large-budded, and multiply budded cells with or without mitochondria in buds. The percentage of cells in each class is shown ($n > 400$).
*The strains used were JSY999 (wild type), JSY1065 (*mdm20Δ*), and JSY707 (*tpm1Δ*).
‡*mdm20Δ* cells carrying the *GAL1-TPM2* plasmid were grown in SGal − Ura medium. The mitochondrial inheritance defect was not affected by growth in galactose media (not shown).

and segregated 2:2 in backcrosses with the wild-type parent strain. 17 of these strains fell into ten complementation groups designated *mdm20-mdm29*; the remaining mutation was a new allele of the previously characterized gene *MDM2*/*OLE1* (Stukey et al., 1989, 1990; Stewart and Yaffe, 1991). In all but one mutant (*mdm29*), the temperature-sensitive growth defects were linked to the defects in mitochondrial distribution and morphology. The *MDM20* complementation group, defined by seven mutant alleles, was chosen for further study.

Wild-type strains grown at 25° or 37°C (Fig. 2, *A* and *B*) segregate a portion of the mitochondrial network into buds almost as soon as they can be detected on the surface of the mother cell. In contrast, *mdm20* mutants retained their branched mitochondrial networks but produced large buds that lack this organelle (Fig. 2, *C* and *D*). This mitochondrial inheritance defect was observed at the permissive temperature and became more pronounced at 37°C (Table II). Both transmission EM and DAPI staining of mitochondrial genomes confirmed that mitochondria were absent from *mdm20* buds (data not shown). In addition, organelles labeled with a mitochondrially targeted form of the green fluorescent protein (kindly provided by R. Jensen) also failed to be transported into buds in the *mdm20* strain (data not shown). Although the *mdm20* mutation caused a striking mitochondrial inheritance defect, it did not severely affect metabolic functions of mitochondria since they could still be efficiently labeled with the potential-dependent dye $DiOC_6$, which only stains actively respiring organelles (Pringle et al., 1989).

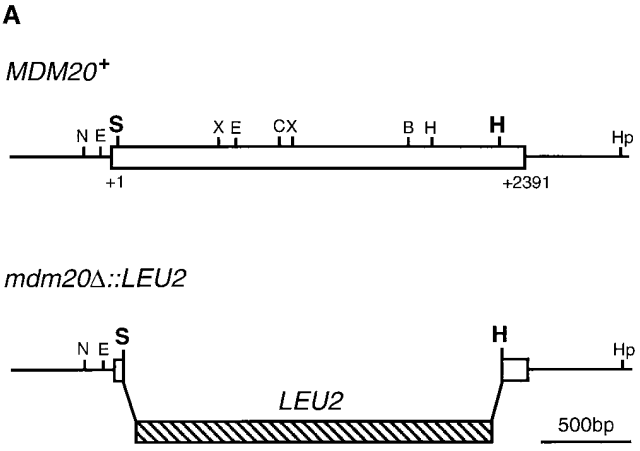

B

```
*
MSDKIQEEILGLVSRSNFKQCYAKLGQLQKQFPNALYFKILETYVKFKQS  50
PGKFDYNKLLEEPYGLKGTTITGDTRSLEFLHNFFVELGKYDEALHVYER 100
GNFKFPSYELSYHWFMKALEDSNYNQMSKASLQLAKYSDSGNLPKRAYYF 150
WNAISILAVSRFQENTLSDPKKILLSRLARQSLLDLKPFQNVQEIIVYCL 200
VLDELFPQSREISEEIVAITFANFDTSVNLYLKNFILKHTKLLNSPQKLF 250
EVCSKLIEKGLDDYELITNLIDAAYKLSKSKDEVKQWIDENLGDSRNTRL 300
ARLKLDIMYTDSVSESSLSYYLSKYHNKPCCSIDLNHYSGHINIDMLKSI 350
MSKYDPEDKDLIHHCNILELGLIGSDSINNYNKFKGTLEKKSVTDYSSCS 400
TFLLEIVKDKCKKTNPELKDVLLCITILENYQAKDPHNFDTMCWLIVLYM 450
YLGLVPDAYFHFINLKIKNVQTDSLDYMIFSRFSTLFPNKQSDFYSKTFH 500
EHNNLYDTSLANLPRYIQVAFERNSYSKILGMLEMRDKLMKSYTRWTKTL 550
ENLQFSRLCNDKRGHLLQKLHEDWRSLEMTQSVSFSDNRDFSILDENFAQ 600
FLNRGKILEYANLNEESIFLTLIRELIIEALPNGEKTEQISALLKKLPSI 650
NLEELLNNNLTEVESASFLIFFEIYENNGKNLHDLISRLMKVPINAKQNW 700
MVSHTYLTKMATLKTLDSLKRIKDKEIQKLIKNSLKELRSCCDDVFKGYS 750
KALVQAYEELKKDECGNLLKELDVKAENVKNIKNSLLGIQKSVRNL     796
```

Figure 3. MDM20 encodes a novel 93-kD protein. (*A*, *top*) Restriction map of the *MDM20* gene (*open box*). (*A*, *bottom*) The *LEU2* construct used to generate the *MDM20* disruption that replaces 2,219 bp (codons 12–751) of the *MDM20* coding region. All restriction enzyme sites in the *MDM20* gene are indicated: *B*, BglII; *C*, ClaI; *E*, EcoRI; *H*, HindIII; *Hp*, HpaI; *S*, SpeI; and *X*, XbaI. (*B*) Predicted amino acid sequence (*single letter code*) of the Mdm20p. The sequence begins at the first potential initiating methionine (*asterisk*). Indicated in boldface are two putative heptad repeats predicted by the COILS 2.1 program (Lupas et al., 1991). These sequence data are available from GenBank/EMBL/DDBJ under accession number U54799.

Isolation and Sequence Analysis of the MDM20 Gene

The *MDM20* gene was isolated by complementing the temperature-sensitive growth defect of the *mdm20-1* mutant allele (see Materials and Methods). Integrative mapping studies indicated that the cloned DNA contained the wild-type *MDM20* gene. Transposon mutagenesis (Sedgwick and Morgan, 1994) and DNA sequence analysis revealed that a 3.2-kb fragment (Fig. 3 *A*) was sufficient to rescue both the temperature-sensitive growth defect (Fig. 4) and the mitochondrial inheritance defect (not shown) in the *mdm20* mutant strain.

The *MDM20* gene predicts a novel, hydrophilic protein that contains 796 amino acids with a calculated molecular mass of 92,821 daltons (Fig. 3 *B*). The sequences adjacent

Table III. Nuclear Segregation in mdm20 and tpm1 Mutants

Genotype/(Plasmid)*	°C				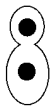			
Wild type	25	56	20	7	17	0	0	0
Wild type	37	52	26	10	12	0	<1	0
mdm20Δ	25	36	23	6	35	0	<1	0
mdm20Δ	37	28	37	2	27	1	5	<1
mdm20Δ + (pRS426-*TPM1*)	25	51	25	6	18	0	0	0
mdm20Δ + (pRS426-*TPM1*)	37	40	34	8	18	0	<1	0
mdm20Δ + (*GAL1-TPM2*)‡	25	46	31	8	15	0	0	0
mdm20Δ + (*GAL1-TPM2*)	37	44	27	9	17	0	3	0
tpm1Δ	25	35	24	6	22	0	13	0
tpm1Δ	37	36	26	9	13	0	16	0

Nuclear inheritance scored in log-phase cells grown at 25° or 37°C for 3 h. The cartoons depict classes scored. The percentage of cells in each class is shown ($n > 400$).
*The strains used were JSY999 (wild type), JSY1065 (*mdm20Δ*), and JSY707 (*tpm1Δ*).
‡*mdm20Δ* cells carrying the *GAL1-TPM2* plasmid were grown in SGal − Ura media. The nuclear inheritance defect was not affected by growth in galactose medium.

to the first potential initiating methionine (Fig. 3 *B*, *asterisk*) fit the consensus for a translational initiation site in yeast (Cigan and Donahue, 1987). Moreover, we demonstrated that an in-frame epitope tag (HA) inserted immediately downstream of this methionine is translated and can be detected on a Western blot (data not shown). Comparison of the Mdm20 protein sequence with all available databases using the FASTA (Pearson and Lipman, 1988), BLAST (Altschul et al., 1990), and Prosite (Bairoch et al., 1995) algorithms revealed no significant homologies with other proteins. However, two potential heptad repeat–containing regions located in the carboxy-terminal portion of the polypeptide are predicted to adopt an α-helical coiled-coil structure (Fig. 3 *B*, *boldface amino acids*). Heptad repeats have been implicated in the homo- and heterodimerization of a variety of proteins with diverse functions (Cohen and Parry, 1986, 1990).

Mdm20p Is Required for Mitochondrial Inheritance during Budding but Does Not Alter Mitochondrial Morphology

Yeast cells harboring *mdm20-1* through *mdm20-7* mutations exhibited defects in mitochondrial inheritance, grew slowly compared to wild type at 25°C, and were dead at 37°C. To further evaluate the role of *MDM20* in vivo, we generated a null allele by replacing codons 12–751 with the *LEU2* gene (Fig. 3 *A*). When diploids heterozygous for the *mdm20::LEU2* null allele were sporulated, dissected into tetrads, and incubated at 25°C, all four spores in each tetrad germinated. However, spores lacking *MDM20* grew slowly and formed small colonies relative to wild type. Further analysis indicated that spores containing the *mdm20::LEU2* disruption did not grow on fermentable (dextrose) or nonfermentable (glycerol) carbon sources at 37°C.

The mitochondrial inheritance defect in the *mdm20::LEU2* cells (*mdm20Δ*) was similar to that observed for the original seven *mdm20* mutant alleles. In log phase cultures grown at 25°C, 14% of *mdm20Δ* mother cells remained attached to buds that failed to inherit mitochondria (Table II). In contrast, mitochondrial segregation defects were not observed in wild-type cultures grown at 25°C (Table II). Incubation at 37°C for 3 h resulted in an increased fraction of *mdm20Δ* cells exhibiting mitochondrial inheritance defects (58%), whereas mitochondrial partitioning in wild-type cells did not change significantly (<1%) (Table II). Moreover, when *mdm20Δ* cells arrested in the unbudded stage were released upon temperature shift, >90% of the buds that formed at 37°C did not inherit mitochondria (data not shown). Despite the severe defect in mitochondrial transmission to buds, $DiOC_6$-stained mitochondrial networks appeared wild type in the *mdm20Δ* cells at both 25°C (98% wild type) and 37°C (95% wild type) (see Fig. 2 *D*). Thus, *MDM20* is required for normal mitochondrial inheritance in yeast but does not appear to play an essential role in maintaining the reticulated network of mitochondrial membranes.

Although nuclear inheritance was normal in *mdm20Δ* cells grown at 25°C, a small number (5%) of binucleate cells was observed at 37°C (Table III; discussed below). This defect in nuclear segregation, while significant, is much less severe than the defect in mitochondrial inheritance in the *mdm20* mutant. We also examined the distribution of the vacuole in the *mdm20* mutant. We found that, at both 25° and 37°C, new *mdm20Δ* buds contained vacuolar material even when mitochondria were absent from the buds (data not shown). Thus, mutations in the *mdm20* gene appear to have the most dramatic affect on inheritance of the mitochondrial compartment.

Extra Copies of Genes Encoding the Actin Binding Proteins Tpm1p and Tpm2p Partially Rescue Mitochondrial Inheritance Defects and Temperature-sensitive Growth Defects in the mdm20 Mutant

To identify loci that interact genetically with *MDM20* and to learn more about the role of the Mdm20 protein, we analyzed multicopy suppressors of the *mdm20-1* temperature-sensitive growth defect. The multicopy suppressors

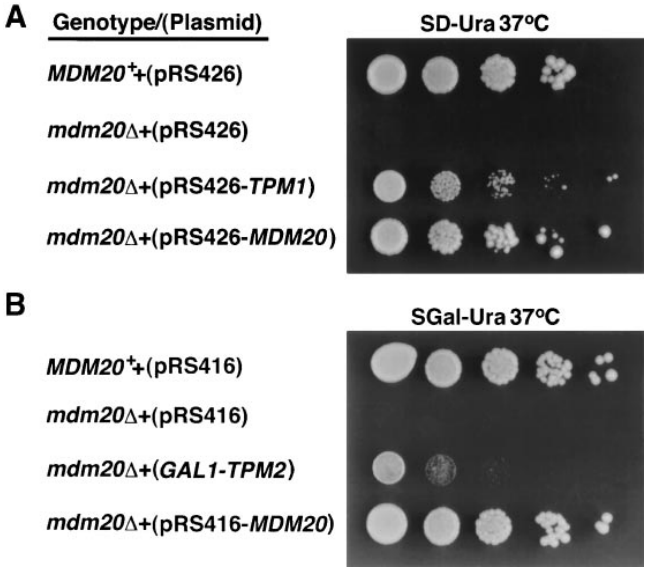

Figure 4. Extra copies of *TPM1* and *TPM2* can suppress the temperature-sensitive growth defect in *mdm20Δ* cells. (*A*) *MDM20*$^+$ (JSY999) or isogenic *mdm20Δ* (JSY1065) strains harboring pRS426, pRS426-*MDM20*, or pRS426-*TPM1* plasmids were serially diluted and spotted on SD minus uracil (*SD − Ura*) solid medium and grown at 37°C for 3 d. (*B*) *MDM20*$^+$ (JSY999) or isogenic *mdm20Δ* (JSY1065) strains harboring pRS416, pRS416-*MDM20*, or *GAL1-TPM2* plasmids were serially diluted and spotted on SGal minus uracil (*SGal − Ura*) solid medium and grown at 37°C for 3 d.

were isolated from a genomic library in a centromere-based yeast vector at the same time the *MDM20* gene was cloned (see Materials and Methods). One of the clones we isolated contained *TPM1*, a previously identified gene that encodes the actin binding protein tropomyosin (Liu and Bretscher, 1989). Tropomyosins are rod-shaped coiled-coil dimers that bind along the groove of the actin helix. Skeletal tropomyosin modulates the interaction between actin and myosin during muscle contraction. In yeast, however, tropomyosins are thought to function in the assembly and/or stabilization of actin cables (Liu and Bretscher, 1989; Bretscher et al., 1994). Although *TPM1* is not an essential gene, cells lacking *TPM1* grow slowly, are heterogeneous in size, and are often multinucleate due to defects in aligning the mitotic spindle (Liu and Bretscher, 1992; Palmer et al., 1992; Wang and Bretscher, 1995). Loss of *TPM1* also results in severe defects in actin cytoskeletal organization, most notably the loss of actin cables (see below) (Liu and Bretscher, 1989). In addition to *TPM1*, yeast contain a second tropomyosin encoded by the *TPM2* gene (Drees et al., 1995). Disruption of the *TPM2* gene does not visibly affect the organization of the actin cytoskeleton and does not hamper cell growth (Drees et al., 1995). However, the genetic and biochemical behavior of Tpm2p and the observed synthetic lethality between *tpm1* and *tpm2* mutations indicate that cellular functions of these two proteins overlap (Drees et al., 1995).

Extra copies of the *TPM1* gene provided on a low copy number (not shown) or high copy number plasmid partially rescued the temperature-sensitive lethality in *mdm20Δ* cells grown at 37°C (Fig. 4). In contrast, the conditional lethality of the *mdm20Δ* mutation was completely suppressed by a wild-type copy of the *MDM20* gene (Fig. 4). Extra copies of *TPM1* also suppressed mitochondrial inheritance defects in the *mdm20Δ* strain. In a culture of *mdm20Δ* cells harboring *TPM1* on a multicopy plasmid, the fraction of cells lacking mitochondria in buds was reduced from 14% to 2% at 25°C and from 58% to 17% at 37°C (Table II). These results indicated that the Tpm1 protein could functionally substitute for the loss of the Mdm20 protein.

To determine whether functional overlaps also existed between Mdm20p and Tpm2p, we asked whether extra copies of *TPM2* could rescue mutant phenotypes in *mdm20Δ* cells. As shown in Fig. 4, the temperature-sensitive growth defect of *mdm20Δ* cells was partially suppressed when Tpm2p was overexpressed from the *GAL1* promoter (Fig. 4 *B*). Overexpression of Tpm2 was also sufficient to reduce the mitochondrial inheritance defect in *mdm20Δ* from 14% to 9% at 25°C and from 58% to 34% at 37°C (Table II). Thus, Mdm20p and Tpm2p apparently have some overlapping functions as well.

MDM20 Is Essential for the Integrity of Actin Cables in Yeast

Taken together, the data presented above suggested that (*a*) *MDM20* and *TPM1* participate in overlapping, essential cellular functions; and (*b*) Tpm2p can partially substitute for Mdm20p when overexpressed. Given what is known about the function of tropomyosins (Pittenger et al., 1994), these results also suggested that the integrity of the actin cytoskeleton is important for mitochondrial inheritance during yeast budding, and that the *mdm20* mutation affects the assembly or organization of F-actin. To further investigate this possibility, we examined the actin cytoskeleton in *mdm20* null cells by rhodamine-phalloidin staining. At both 25° and 37°C, wild-type cells contained well-defined actin cables and cortical actin patches concentrated in growing buds (Fig. 5, *A–D*). In contrast, actin cables were absent in 100% of the *mdm20* null cells examined at

Table IV. Synthetic Lethal Relationship Involving mdm20

Cross	Segregation pattern*			Double mutants
	PD	TT	NPD	*alive:dead*
mdm20Δ::LEU2(JSY1065) × *tpm1Δ::HIS3*(JSY1084)	8	20	5	0:30‡
mdm20Δ::LEU2(JSY1340) × *tpm2Δ::HIS3*(JSY1285	11	48	8	64:0
mdm20Δ::LEU2(JSY1065) × *bem2-10*(ABY249)	8	26	3	0:32§
mdm20Δ::LEU2(JSY1340) × *myo2-66*(SLY63)	12	35	18	0:71‖
mdm20Δ::LEU2(JSY1340) × *sac6Δ::LEU2*(IGY4)	2	5	2	9:0

*The segregation patterns for *mdm20Δ::LEU2*, *tpm1Δ::HIS3*, *tpm2Δ::HIS3*, *bem2-10* (enlarged cells), *myo2-66* (t.s.), and *sac6Δ::LEU2* are shown (*PD*, parental ditype; *TT*, tetratype; *NPD*, nonparental ditype). In cases where synthetic lethality was observed, the segregation pattern was inferred from other viable members of the tetrad.
‡*mdm20Δtpm1Δ* double mutants form terminal microcolonies containing 50–100 cells.
§*mdm20Δbem2-10* double mutants form terminal microcolonies containing 20–40 cells.
‖*mdm20Δmyo2-66* double mutants form terminal microcolonies containing 100–500 cells.

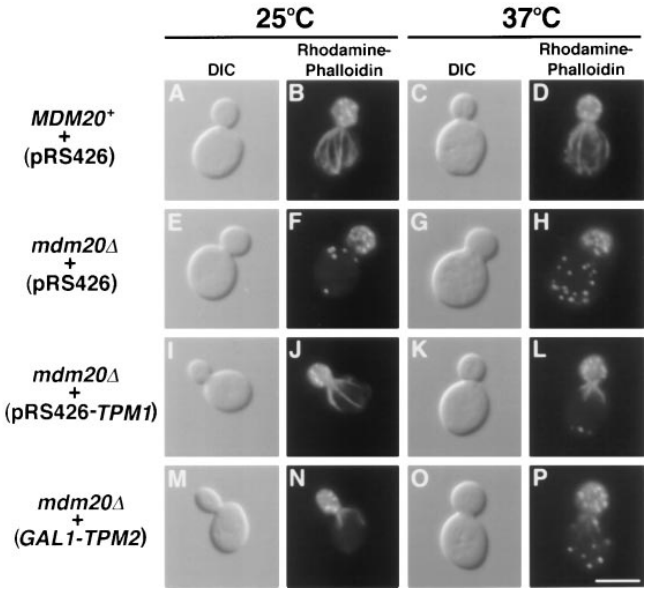

Figure 5. Actin cables lacking in *mdm20Δ* cells are partially restored by introducing extra copies of *TPM1* and *TPM2*. *MDM20*$^+$ cells (JSY999) carrying pRS426 (*A–D*) and *mdm20Δ* cells (JSY1065) carrying pRS426 (*E–H*), pRS426-*TPM1* (*I–L*), or GAL1-*TPM2* (*M–P*) were grown in SD − Ura or SGal − Ura at 25°C, and then shifted to 25° and 37°C for 3 h. Cells were stained with rhodamine-phalloidin and visualized by DIC or fluorescence microscopy as indicated. Representative cells are shown. Bar, 5 μm.

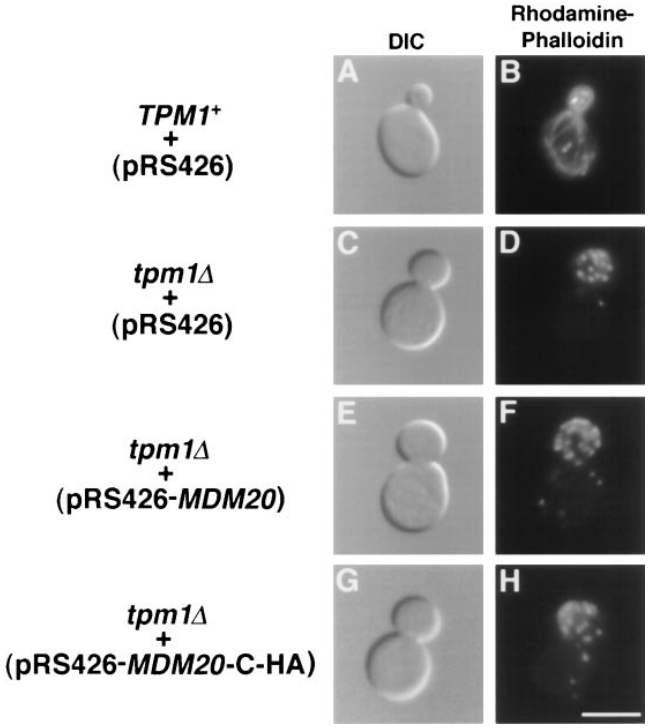

Figure 6. Actin cables lacking in *tpm1Δ* cells are not restored by overexpression of Mdm20p. *TPM1*$^+$ cells (FY22) containing pRS426 (*A* and *B*) and *tpm1Δ* cells (JSY707) containing pRS426 (*C* and *D*), pRS426-*MDM20* (*E* and *F*), or pRS426-*MDM20*-C-HA (*G* and *H*) were grown at 25°C, stained with rhodamine-phalloidin, and visualized by DIC or fluorescence microscopy as indicated. Representative cells are shown. Bar, 5 μm.

both temperatures (Fig. 5, *E–H*). *mdm20Δ* cells were able to divide, however, and contained brightly staining cortical patches that were predominantly clustered in buds at 25°C (Fig. 5, *E* and *F*; >95% of cells) and partially delocalized at 37°C (Fig. 5, *G* and *H*; >50% of cells). The fact that mitochondrial inheritance defects are already present at 25°C in the *mdm20* mutant (at a temperature where patches are still properly localized) suggests that it is the disruption of actin cables that is primarily responsible for the lack of mitochondrial transmission.

Rhodamine-phalloidin staining also revealed that multiple copies of *TPM1* restored actin cable formation in the *mdm20* mutant. At 25°C, >95% of the *mdm20* cells containing *TPM1* on a multicopy plasmid had actin cables that were robust and extended the full length of the mother cell (Fig. 5, *I* and *J*). However, these restored cables appeared fewer in number than those observed in wild type. At 37°C, >95% of *mdm20* cells also contained the *TPM1*-restored cables. However, these cables were shorter than normal, and, while visible near the mother-bud neck, they rarely extended the full length of the mother cell (Fig. 5, *K* and *L*). The delocalization of actin cortical patches in *mdm20Δ* cells at 37°C was also rescued by introducing extra copies of *TPM1* (Fig. 5, *K* and *L*; >95% of cells). Abbreviated actin cables were also observed in >90% of the *mdm20Δ* cells overexpressing Tpm2p from the *GAL1* promoter at 25°C (Fig. 5, *M* and *N*). At 37°C, only faint cables were observed near the mother-bud neck in *mdm20Δ* cells containing *GAL1-TPM2* (Fig. 5, *O* and *P*; >90% of cells). Finally, the wild-type *MDM20* gene on a low copy number plasmid was able to completely restore cables in >98% of *mdm20Δ* cells (data not shown). This partial restoration of actin cables and mitochondrial inheritance by *TPM1* and *TPM2* was striking and suggested that the defect in mitochondrial inheritance observed in *mdm20* is linked to the loss of actin cables in these cells.

MDM20 Fails to Complement Mutant Phenotypes in tpm1Δ Cells

Although overexpression of *TPM1* suppressed mitochondrial inheritance defects and restored actin cables in the *mdm20* mutant, the functions of the Tpm1 and Mdm20 proteins were not completely interchangeable. As shown in Fig. 6, *C* and *D*, and reported previously, actin cables are absent in *tpm1Δ* mutant cells (Liu and Bretscher, 1989). However, actin cables could not be restored by introducing extra copies of the *MDM20* gene into *tpm1Δ* cells on a high copy number plasmid (Fig. 6, *E* and *F*) or by overexpressing epitope-tagged versions of the Mdm20p (Fig. 6, *G* and *H*; data not shown). In the latter experiments, Mdm20p overexpression was monitored using amino- and carboxy-terminal HA-tagged Mdm20 proteins (see Materials and Methods). Wild-type cells containing Mdm20p-C-HA on a centromere-based plasmid expressed relatively low levels of the tagged protein (Fig. 7, lane *3*). The steady state protein level increased more than eightfold when Mdm20-C-HA protein was expressed from a multicopy plasmid (Fig. 7, lane *4*). Identical results were obtained when expression of the Mdm20p-N-HA was examined in wild-type cells (data

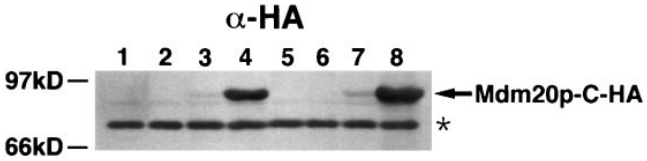

Figure 7. Expression of Mdm20p-C-HA in wild-type and *tpm1Δ* cells. Extracts were prepared from wild-type cells (JSY999) containing pRS416 (lane *1*), pRS426 (lane *2*), pRS416-*MDM20*-C-HA (lane *3*), and pRS426-*MDM20*-C-HA (lane *4*), or *tpm1Δ* cells (JSY707) containing pRS416 (lane *5*), pRS426 (lane *6*), pRS416-*MDM20*-C-HA (lane *7*), and pRS426-*MDM20*-C-HA (lane *8*). The cells were harvested after growth to mid log phase at 25°C, and equal amounts (equivalent OD units) of the cell extracts were subjected to SDS-PAGE and transferred to nitrocellulose. The nitrocellulose was probed with antibodies to the HA epitope. The arrowhead identifies the Mdm20-C-HA protein, and the asterisk identifies a background band that was used to normalize the amount of protein present in each lane.

not shown). Fusion of the HA tag to the Mdm20 protein had no obvious effects on its function, as these constructs completely rescued temperature-sensitive growth defects, mitochondrial inheritance defects, and loss of actin cables in *mdm20* mutant strains (data not shown). Furthermore, overexpression of HA-tagged Mdm20p constructs did not induce additional phenotypes in wild-type cells (data not shown). We found that *tpm1Δ* cells overexpressing Mdm20p (Fig. 7, lane *8*) did not grow significantly better than *tpm1Δ* cells alone. In addition, overexpression of Mdm20p did not rescue the lethality observed in *tpm1Δ tpm2Δ* double mutants. Together, these findings suggest that *MDM20* cannot bypass the requirement for Tpm1p and Tpm2p in cells. Furthermore, although expression of Tpm1p in wild-type cells results in thicker actin cables (Liu and Bretscher, 1989), the actin cytoskeleton was not affected by overexpressing Mdm20p in a wild-type strain (data not shown). Thus, Mdm20p and Tpm1p appear to perform some distinct functions in cells.

Loss of Actin Cables in mdm20Δ and tpm1Δ Cells Disrupts Mitochondrial Inheritance and Nuclear Segregation to Different Extents

To further evaluate functional overlaps between Mdm20p and Tpm1p, we examined mitochondrial inheritance and morphology in the *tpm1Δ* mutant. Although actin cables are also absent in *tpm1Δ* cells, we were surprised to find that *tpm1* null strains did not exhibit significant defects in mitochondrial inheritance at 25° (<1%) or 37°C (5%) (Table II). In addition, mitochondrial morphology appeared normal in *tpm1Δ* cells at both temperatures (99% wild type at 25°C and 96% wild type at 37°C). The mitochondrial inheritance phenotype of *tpm1Δ* contrasted with that of *mdm20* null cells, which displayed more severe defects in mitochondrial inheritance at both temperatures (14% at 25°C and 58% at 37°C; Table II). These phenotypic differences, together with the results described above, supported the notion that the Mdm20 and Tpm1 proteins perform some distinct roles in cells. To extend these observations, we examined nuclear segregation (a process known to be defective in *tpm1* mutants) in isogenic *tpm1* and *mdm20* strains.

During division, the mitotic spindle is oriented by interactions of astral microtubules with the actin cytoskeleton. Disruption of this interaction in *act1* mutants results in misoriented spindles that give rise to binucleate cells (Palmer et al., 1992). Consistent with previous reports (Liu and Bretscher, 1989; Wang and Bretscher, 1995), we found that *tpm1Δ* mutants lacking actin cables exhibited nuclear segregation defects and produced a significant proportion of multinucleate cells at 25°C (13%) and 37°C (16%) (Table III). Conversely, nuclear segregation was wild type in *mdm20Δ* cells grown at 25°C, although a small number (5%) of binucleate cells was observed at 37°C (Table III). Extra copies of *TPM1* (but not overexpression of Tpm2p) suppressed the formation of binucleate cells at 37°C in the *mdm20Δ* strain (Table III). Thus, *tpm1* mutants displayed more severe defects in nuclear segregation than *mdm20* mutants. Together, these data indicate that, although *TPM1* and *MDM20* are both required for the formation and/or stabilization of actin cables, their roles in cellular processes such as mitochondrial inheritance and nuclear segregation differ significantly.

Null Mutations in mdm20 are Synthetically Lethal With Mutations in tpm1, myo2, and bem2

Although *TPM1* and *TPM2* null mutants are alive at 25°C, the combinatorial loss of these two genes in a haploid strain results in cell death (Drees et al., 1995). This synthetic lethality is thought to arise because Tpm1p and Tpm2p carry out some redundant functions required for an essential cellular process (Drees et al., 1995). The similar actin phenotypes we observed in *tpm1* and *mdm20* mutants prompted us to genetically test the possibility that *MDM20* acts in a common pathway with tropomyosins. The phenotypes of haploid *mdm20Δ tpm1Δ* and *mdm20Δ tpm2Δ* double mutants were examined after dissecting tetrads generated from diploid cells heterozygous for null mutations in both *MDM20* and *TPM1.* In 33 tetrads analyzed, double *mdm20Δ tpm1Δ* mutants were never observed (30 expected; Table IV). Although *mdm20Δ tpm1Δ* spores germinated, they were defective in mitotic growth and gave rise to microcolonies of 50–100 cells that could not be analyzed further. These results were confirmed by repeating the cross with an *mdm20Δ* strain carrying the wild-type *MDM20* gene on a *URA3*-marked plasmid. In this experiment, *mdm20Δ tpm1Δ* cells harboring the *MDM20 URA3* plasmid were recovered and were viable unless forced to lose the plasmid on 5-FOA plates (data not shown). Synthetic lethal interactions were not observed between *MDM20* and *TPM2* in similar crosses (Table IV), and mitochondrial inheritance and morphology defects were not observed in *tpm2Δ* cells (data not shown).

Previous studies indicated that *tpm1* also exhibits synthetic growth defects with mutations in *BEM2* (Wang and Bretscher, 1995) and *MYO2* (Liu and Bretscher, 1992). The *BEM2* gene encodes a GTPase-activating protein required for bud emergence, a process that involves polarization of actin cables and patches to the site of bud growth (Kim et al., 1994; Peterson et al., 1994). *MYO2* encodes a type V myosin family member that forms a cap at or near the plasma membrane on unbudded cells and small buds (Johnston et al., 1991; Lillie and Brown, 1994). In crosses

similar to those described above, we determined that mutations in *BEM2* and *MYO2* are also synthetically lethal with *mdm20* (Table IV). We also examined synthetic interactions between mutations in *MDM20* and the *SAC6* gene that encodes the actin cross-linking protein, fimbrin (Adams et al., 1991). Although Sac6p, like Tpm1p, localizes to actin cables in wild-type yeast cells, synthetic growth defects were not detected for *tpm1 sac6* double mutants (Adams et al., 1993) and were not observed in crosses we performed with *mdm20* and *sac6* mutant strains (Table IV). Thus, *mdm20* and *tpm1* mutants not only exhibit similar actin organization defects but also show the same pattern of genetic interactions.

Discussion

We have demonstrated that the *MDM20* gene encodes a novel protein required for proper mitochondrial segregation in yeast. Cells lacking Mdm20p are temperature sensitive for growth and fail to transport mitochondria into newly formed buds. Our results indicate that the defect in the *mdm20* mutant specifically disrupts mitochondrial transport but not mitochondrial morphology in these cells. In addition, the *mdm20* mutation does not severely interrupt the division and segregation of the nucleus, and other cytoplasmic organelles, such as vacuoles, are always detected in *mdm20* daughter cells that fail to inherit the mitochondrial compartment. Together, our findings establish an essential role for *MDM20* in mitochondrial partitioning during mitotic division.

Two different cytoskeletal elements in yeast, actin (Drubin et al., 1993; Lazzarino et al., 1994) and an intermediate filament–like protein (McConnell and Yaffe, 1992), have been proposed to play a central role in mitochondrial inheritance. In this study we present two lines of in vivo evidence that mitochondrial inheritance in yeast is an actin-mediated process. First, two major phenotypic consequences of disrupting *MDM20* appear to be the cessation of mitochondrial movement into buds during division and the loss of observable actin cables in cells. Second, overexpression of two well-characterized actin binding proteins, Tpm1p and Tpm2p, suppresses temperature-sensitive growth and mitochondrial inheritance defects and partially restores actin cables in the *mdm20* mutant. Although it is possible that Mdm20p fulfills distinct functions in mitochondrial inheritance and actin cable organization, the observation that overexpression of Tpm1p and Tpm2p can partially rescue defects in both processes in *mdm20* mutants suggests that these two phenotypes cannot be separated from one another. Moreover, a direct link between mitochondrial segregation and the actin cytoskeleton is consistent with the recent observations that yeast mitochondria colocalize with actin cables in vivo (Drubin et al., 1993), can bind to phalloidin-stabilized actin filaments in vitro (Lazzarino et al., 1994), and contain an actin-dependent myosin-like motor activity on their surface (Simon et al., 1995). Thus, our data strongly support a model in which mitochondria are transported into yeast buds along polarized actin filaments or cables.

The organization and stabilization of the actin cytoskeleton in yeast depends on the activities of a large number of actin binding proteins and regulatory factors. Mdm20p is a new member of this important group of proteins required for the integrity of actin cables in cells. Previous studies indicate that defects in actin organization cause a variety of phenotypes including temperature-sensitive lethality, osmotic sensitivity, and defects in cell morphology, mitochondrial dynamics, secretion, endocytosis, and nuclear segregation (for review see Bretscher et al., 1994; Welch et al., 1994). In addition to the phenotypes we have reported here for the *mdm20* mutant, our preliminary studies suggest that *mdm20* cells are rounder than wild type and heterogeneous in size, exhibit defects in chitin localization, and accumulate small vesicles (unpublished observations). These data provide further support that *MDM20* is required for normal functions of the actin cytoskeleton. Most importantly, *MDM20* defines a new class of genes that control both actin organization and mitochondrial transport during division.

Previous studies of the actin–myosin complex identified a myosin "footprint" on the actin monomer (Rayment et al., 1993; Schroder et al., 1993). Charge-to-alanine substitutions located under the equivalent myosin footprint in the yeast actin monomer have been shown to cause defects in mitochondrial morphology, specifically mitochondrial aggregation (Drubin et al., 1993). The mutants with aberrant mitochondrial morphology exhibit severe actin organization defects that are most pronounced at 37°C, including loss of actin cables and/or patches, delocalized patches, and reduced or faint cables. In contrast, we find that *mdm20* mutants lacking actin cables exhibit disrupted mitochondrial transport but not mitochondrial morphology. Similarly, we do not observe defects in mitochondrial morphology in isogenic *tpm1* mutant cells. If the actin cytoskeleton plays a role in regulating mitochondrial morphology, then the structures required must still be present in *mdm20* and *tpm1* mutant cells. Alternatively, other cytoplasmic structures or cytoskeletal proteins may be responsible for controlling yeast mitochondrial morphology.

Our observation that mitochondrial morphology and inheritance is normal in the *tpm1Δ* mutant is interesting in light of previous reports that *tpm1Δ* strains generate petites (lose mitochondrial genome function) at a higher frequency than wild type (Liu and Bretscher, 1992). We also find that *mdm20Δ* and *tpm1Δ* cells generate petites at a high frequency when maintained on dextrose. One possible explanation for these results is that *tpm1* daughter cells frequently receive DNA-free mitochondrial compartments. In our experiments, mitochondrial morphology and distribution were measured by labeling the mitochondrial compartment with the potential dependent dye, $DiOC_6$, and labeling mtDNA nucleoids with DAPI. We observed that *tpm1Δ* cells segregated both the mitochondrial compartment (Table II) and mitochondrial nucleoids (data not shown) into daughter cells. Furthermore, we did not detect a large number of *tpm1* cells lacking mt nucleoids. Thus, the increased petite formation in *tpm1* cells is not simply the result of a block in mtDNA transfer to buds. Further experiments are required to determine the mechanism by which these strains become petite.

Some of our studies suggest that Tpm1p and Mdm20p might perform overlapping functions required for the integrity of the actin cytoskeleton. The disruption of both genes causes a similar loss of actin cables in cells and com-

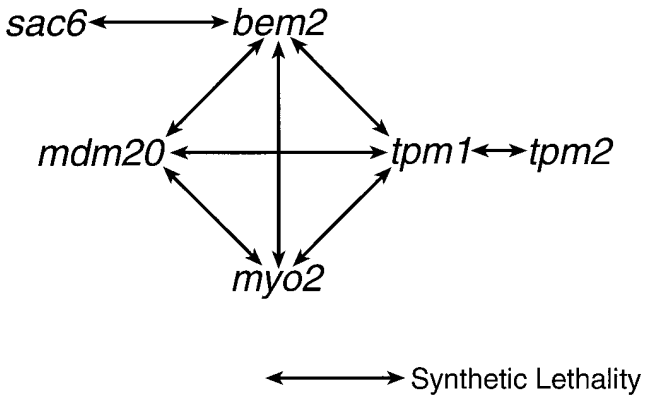

Figure 8. Summary of the synthetic interactions that involve *mdm20.* The synthetic interactions between *tpm1* and *bem2* (Wang and Bretscher, 1995), *myo2* (Liu and Bretscher, 1992), and *tpm2* (Drees et al., 1995) were previously reported.

binations of mutations in *MDM20* and *TPM1* result in synthetic lethality. In addition, like *tpm1*, *mdm20* exhibits synthetic growth defects in combination with mutations in either *BEM2* or *MYO2* but not *SAC6* (Fig. 8). Furthermore, we observe that overexpression of Tpm1p restores actin cables and rescues mitochondrial inheritance defects in *mdm20.* However, this suppression is not reciprocal; overexpression of Mdm20p does not rescue mutant phenotypes in *tpm1* cells, suggesting that their roles in organizing actin differ. Mdm20p and Tpm1p do not appear to be structurally homologous since their amino acid sequences and sizes are quite different. If Mdm20p and Tpm1p do not have redundant functions, then an alternative explanation for the rescue of *mdm20* mutant phenotypes by overexpressed Tpm1p is required. One possibility is that the overexpression of Tpm1p leads to the global stabilization of all actin filaments and cables in *mdm20* cells, including those necessary for mitochondrial transport and inheritance. In support of this model, overexpression of Tpm1p is reported to cause more prominent cables and actin networks in wild-type cells and can restore actin cables in *act1-2* mutant strains (Liu and Bretscher, 1989). Although overexpression of Tpm2p also suppresses mutant phenotypes in *mdm20*, we did not observe synthetic lethality in *mdm20 tpm2* double mutants. Previous studies showed that the level of Tpm2p expression in wild-type cells is much lower than that of Tpm1p, and that cells lacking *TPM2* do not exhibit defects in actin organization or growth (Drees et al., 1995). Thus, *mdm20Δ tpm2Δ* cells may contain enough Tpm1p to compensate for the loss of Tpm2p and prevent the cell death observed in *mdm20Δ tpm1Δ* double mutants.

Interestingly, although mutations in *MDM20* and *TPM1* cause similar defects in actin organization, the mutant phenotypes in these two strains are distinct. *mdm20Δ* mutant cells exhibit severe defects in mitochondrial inheritance (58%) and only slight defects in nuclear segregation (5%). Conversely, *tpm1Δ* strains exhibit weak defects in mitochondrial inheritance (5%) and stronger defects in nuclear segregation (16%). As discussed above, while overexpression of Tpm1p can rescue mutant phenotypes in *mdm20*, the converse is not true. These observations suggest that Mdm20p and Tpm1p perform different roles in vivo and support the hypothesis that there are functionally distinct classes of actin-containing structures in cells. It is important to note that *mdm20* and *tpm1* mutant cells lacking actin cables may contain individual actin filaments that are not detected by rhodamine-phalloidin staining. Thus, actin filaments that play a role in mitochondrial inheritance may be present in the *tpm1* mutant but absent in the *mdm20* mutant. By the same reasoning, actin-containing structures required for nuclear segregation may be more severely disrupted in the *tpm1* mutant than in the *mdm20* mutant. In this way, *MDM20* and *TPM1* could be acting to establish molecular and functional heterogeneity in the actin cytoskeleton.

As illustrated in Fig. 8, our synthetic lethal studies suggest that *MDM20* functions in a cellular process that also requires *TPM1*, *BEM2*, and *MYO2.* Assembly and/or stabilization of the actin cytoskeleton is an obvious candidate for this process since defects in actin organization have been reported for mutations in all of these genes (Liu and Bretscher, 1989; Johnston et al., 1991; Kim et al., 1994; Wang and Bretscher, 1995). The synthetic growth defects we observe between *mdm20* and *tpm1*, *bem2*, and *myo2* may simply reflect the fact that partial defects in actin organization can be tolerated at 25°C, but combinations of defects cannot. However, this interpretation is not supported by the findings that double mutants lacking both *MDM20* and *SAC6* (Table IV and Fig. 8) or *SAC6* and *TPM1* (Adams et al., 1993) are viable. An alternative possibility is that synthetic lethality between mutations in these genes results from a failure to coordinate bud site assembly with the actin polarization required for directed membrane transport and bud growth. Lillie and Brown (1994) have suggested that Myo2p localized at the incipient bud site might function to anchor actin filaments that are required for the polarized delivery of vesicles to the bud. In support of this model, both *myo2* and *tpm1* mutants accumulate small vesicles, and we have observed similar vesicles in a small number of *mdm20* cells (data not shown). Our studies of the *mdm20* mutant indicate that polarized actin cables are also required for the delivery of mitochondria to buds. Physical and genetic interactions reported for *BEM2* suggest that the Bem2p protein may also localize to the bud site where it is postulated to regulate Tpm1p-containing actin filaments (Wang and Bretscher, 1995). Based on the synthetic lethal interactions observed to date, we speculate that viable *mdm20* and *tpm1* cells lacking actin cables still contain some undetected actin filaments that are properly polarized to the bud site. However, when *mdm20* and *tpm1* are combined with mutations in genes that control actin filament polarization to the bud site, synthetic lethality results.

Although *MDM20* encodes a novel protein required for the organization of the actin cytoskeleton, analysis of the predicted Mdm20 amino acid sequence does not reveal any known actin binding domains. Mdm20p does contain two potential heptad repeats, however, which could modulate its homo- or heterodimerization through the formation of α-helical coiled-coils. While the specific biochemical activity of Mdm20p is unknown, it is likely to participate in the assembly or function of actin-containing structures necessary for mitochondrial segregation. In this regard,

Mdm20p could bind directly to filamentous actin or might act in a signaling pathway that directs the assembly or stabilization of actin filaments or cables that transport mitochondria during cell division. We think it is unlikely that Mdm20p is a major structural component of actin filaments or cables for two reasons. First, our studies with the HA-tagged Mdm20p suggest that relatively low levels of the protein are able to completely rescue mutant phenotypes in the *mdm20* strain (see Fig. 7). Second, we have been unable to localize the low abundance of HA-tagged Mdm20p in wild-type or *mdm20* cells (data not shown). In cells overexpressing HA-tagged Mdm20p, the protein is found dispersed throughout the cytoplasm and does not appear to be concentrated along actin cables or at actin patches (data not shown). Based on these results, we suggest that Mdm20p serves a regulatory function in cells. We are currently studying the function of this interesting protein in organizing actin and in directing mitochondrial transport and inheritance.

We are grateful to Drs. Alison Adams, Anthony Bretscher, Susan Brown, John Cooper, Tim Formosa, Edina Harsay, Rob Jensen, Sue Lillie, David Stillman, Fred Winston, and Michael Yaffe for providing strains, antibodies, and plasmids. We especially thank Jason Singer and William Bleazard for the *mdm20*/*sac6* and *mdm20*/*bem2* synthetic lethality data. We also thank David Nix for technical advice, and Drs. Mary Beckerle, Tim Formosa, David Gard, and members of the Shaw laboratory for stimulating discussions and careful review of the manuscript.

This work was supported by grants from the American Cancer Society (CB-97) and the National Institutes of Health (NIH) (GM53466) to J. Shaw. G. Hermann was supported in part by an NIH Predoctoral Genetics training grant and a University of Utah Graduate Research fellowship.

Received for publication 23 October 1996 and in revised form 6 February 1997.

References

Adams, A.E.M., and J.R. Pringle. 1984. Relationship of actin and tubulin distribution in wild-type and morphogenetic mutant *Saccharomyces cerevisiae. J. Cell Biol.* 98:934–945.

Adams, A.E.M., and J.R. Pringle. 1991. Staining of actin with fluorochrome-conjugated phalloidin. *Methods Enzymol.* 194:729–731.

Adams, A.E.M., D. Botstein, and D.G. Drubin. 1991. Requirement of yeast fimbrin for actin organization and morphogenesis *in vivo. Nature (Lond.).* 354:404–408.

Adams, A.E.M., J.A. Cooper, and D.G. Drubin. 1993. Unexpected combinations of null mutations in genes encoding the actin cytoskeleton are lethal in yeast. *Mol. Biol. Cell.* 4:459–468.

Altschul, S.F., W. Gish, W. Miller, E.W. Meyers, and D.J. Lipman. 1990. Basic local alignment search tool. *J. Mol. Biol.* 215:403–410.

Backer, J.S. 1995. New alleles of *mgm1*: a gene encoding a protein with a GTP-binding domain related to dynamin. *Curr. Genet.* 28:499–501.

Bairoch, A., P. Bucher, and K. Hofmann. 1995. The PROSITE database, its status in 1995. *Nucleic Acids Res.* 24:189–196.

Ball, E.H., and S.J. Singer. 1982. Mitochondria are associated with microtubules and not with intermediate filaments in cultured fibroblasts. *Proc. Natl. Acad. Sci. USA.* 79:123–126.

Baudin, A., O. Ozier-Kalogeropoulos, A. Denouel, F. Lacroute, and C. Cullin. 1993. A simple and efficient method for direct gene deletion in *Saccharomyces cerevisiae. Nucleic Acids Res.* 21:3329–3330.

Bereiter-Hahn, J. 1990. Behavior of mitochondria in the living cell. *Int. Rev. Cytol.* 122:1–63.

Bereiter-Hahn, J., and M. Voth. 1994. Dynamics of mitochondria in living cells: shape changes, dislocations, fusion, and fission of mitochondria. *Microsc. Res. Tech.* 27:198–219.

Bretscher, A., B. Drees, E. Harsay, D. Schott, and T. Wang. 1994. What are the basic functions of microfilaments? Insights from studies in budding yeast. *J. Cell Biol.* 126:821–825.

Burgess, S.M., M. Delannoy, and R.E. Jensen. 1994. *MMM1* encodes a mitochondrial outer membrane protein essential for establishing and maintaining the structure of yeast mitochondria. *J. Cell Biol.* 126:1375–1391.

Cigan, A.M., and T.F. Donahue. 1987. Sequence and structural features associated with translational initiator regions in yeast: a review. *Gene (Amst.).* 59: 1–18.

Cohen, C., and D.A.D. Parry. 1986. α-helical coiled coils: a widespread motif in proteins. *Trends Biochem. Sci.* 11:245–248.

Cohen, C., and D.A.D. Parry. 1990. α-helical coiled coils and bundles: how to design an α-helical protein. *Proteins Struct. Funct. Genet.* 7:1–15.

Diffley, J.F., and B. Stillman. 1991. A close relative of the nuclear, chromosomal high-mobility group protein HMG1 in yeast mitochondria. *Proc. Natl. Acad. Sci. USA.* 88:7864–7868.

Diffley, J.F., and B. Stillman. 1992. DNA binding properties of an HMG1-related protein from yeast mitochondria. *J. Biol. Chem.* 267:3368–3374.

Drees, B., C. Brown, B.G. Barrell, and A. Bretscher. 1995. Tropomyosin is essential in yeast, yet the *TPM1* and *TPM2* products perform distinct functions. *J. Cell Biol.* 128:383–392.

Drubin, D.G., H.D. Jones, and K.F. Wertman. 1993. Actin structure and function: roles in mitochondrial organization and morphogenesis in budding yeast and identification of the phalloidin-binding site. *Mol. Biol. Cell.* 4: 1227–1294.

Guan, K., L. Farh, T.K. Marshall, and R.J. Deschenes. 1993. Normal mitochondrial structure and genome maintenance in yeast requires the dynamin-like product of the *MGM1* gene. *Curr. Genet.* 24:141–148.

Hannavy, K., S. Rospert, and G. Schatz. 1993. Protein import into mitochondria: a paradigm for the translocation of polypeptides across membranes. *Curr. Opin. Cell Biol.* 5:694–700.

Harlow, E., and D. Lane. 1988. Antibodies: A Laboratory Manual. Cold Spring Harbor Laboratory, Cold Spring Harbor, NY. 726 pp.

Heggeness, M.H., M. Simon, and S.J. Singer. 1978. Association of mitochondria with microtubules in cultured cells. *Proc. Natl. Acad. Sci. USA.* 75:3863–3866.

Hoffman, H., and C.J. Avers. 1973. Mitochondrion of yeast: ultrastructural evidence for one giant, branched organelle per cell. *Science (Wash. DC).* 181: 749–751.

Hollenbeck, P.J. 1996. The pattern and mechanism of mitochondrial transport in axons. *Front. Biosci.* 1:91–102.

Ito, H., Y. Fukuda, K. Murata, and A. Kimura. 1983. Transformation of intact yeast cells with alkali cations. *J. Bacteriol.* 153:163–168.

Johnston, G.C., J.A. Prendergast, and R.A. Singer. 1991. The *Saccharomyces cerevisiae MYO2* gene encodes an essential myosin for vectorial transport of vesicles. *J. Cell Biol.* 113:539–551.

Jones, B.A., and W.L. Fangman. 1992. Mitochondrial DNA maintenance in yeast requires a protein containing a region related to the GTP-binding domain of dynamin. *Genes & Dev.* 6:380–389.

Kilmartin, J., and A.E.M. Adams. 1984. Structural rearrangements of tubulin and actin during the cell cycle of the yeast *Saccharomyces. J. Cell Biol.* 98: 922–933.

Kim, Y., L. Francisco, G. Chen, E. Marcotte, and C.S.M. Chan. 1994. Control of cellular morphogenesis by the Ipl2/Bem2 GTPase-activating protein: possible role of protein phosphorylation. *J. Cell Biol.* 127:1381–1394.

Koning, A.J., P.Y. Lum, J.M. Williams, and R. Wright. 1993. $DiOC_6$ staining reveals organelle structure and dynamics in living yeast cells. *Cell Motil. Cytoskeleton.* 25:111–128.

Kubrich, M., K. Dietmeier, and N. Pfanner. 1995. Genetic and biochemical dissection of the mitochondrial protein-import machinery. *Curr. Genet.* 27: 393–403.

Kuznetsov, S.A., G.M. Langford, and D.G. Weiss. 1992. Actin-dependent organelle movement in squid axoplasm. *Nature (Lond.).* 356:722–725.

Lazzarino, D.A., I. Boldogh, M.G. Smith, J. Rosand, and L.A. Pon. 1994. Yeast mitochondria contain ATP-sensitive, reversible actin-binding activity. *Mol. Biol. Cell.* 5:807–818.

Lill, R., and W. Neupert. 1996. Mechanisms of protein import across the mitochondrial outer membrane. *Trends Cell Biol.* 6:56–61.

Lillie, S.H., and S.S. Brown. 1994. Immunofluorescence localization of the unconventional myosin, Myo2p, and the putative kinesin-related protein, Smy1p, to the same regions of polarized growth in *Saccharomyces cerevisiae. J. Cell Biol.* 125:825–842.

Liu, H., and A. Bretscher. 1989. Disruption of the single tropomyosin gene in yeast results in the disappearance of actin cables from the cytoskeleton. *Cell.* 57:233–242.

Liu, H., and A. Bretscher. 1992. Characterization of *TPM1* disrupted yeast cells indicates an involvement of tropomyosin in directed vesicular transport. *J. Cell Biol.* 118:285–299.

Lupas, A., M. Van Dyke, and J. Stock. 1991. Predicting coiled coils from protein sequences. *Science (Wash. DC).* 252:1162–1164.

Maniatis, T., E.F. Fritsch, and J. Sambrook. 1982. Molecular Cloning: A Laboratory Manual. Cold Spring Harbor Laboratory, Cold Spring Harbor, NY. 545 pp.

McConnell, S.J., and M.P. Yaffe. 1992. Nuclear and mitochondrial inheritance in yeast depends on novel cytoplasmic structures defined by the MDM1 protein. *J. Cell Biol.* 118:385–395.

McConnell, S.J., and M.P. Yaffe. 1993. Intermediate filament formation by a yeast protein essential for organelle inheritance. *Science (Wash. DC).* 260: 687–689.

McConnell, S.J., L.C. Stewart, A. Talin, and M.P. Yaffe. 1990. Temperature-sensitive yeast mutants defective in mitochondrial inheritance. *J. Cell Biol.* 111:967–976.

Morris, R.L., and P.J. Hollenbeck. 1995. Axonal transport of mitochondria

along microtubules and F-actin in living vertebrate neurons. *J. Cell Biol.* 131: 1315–1326.
Mose-Larsen, P., R. Bravo, S.J. Fey, J.V. Small, and J.E. Celis. 1982. Putative association of mitochondria with a subpopulation of intermediate-sized filaments in cultured human skin fibroblasts. *Cell.* 31:681–692.
Mulholland, J., D. Preuss, A. Moon, A. Wong, D. Drubin, and D. Botstein. 1994. Ultrastructure of the yeast actin cytoskeleton and its association with the plasma membrane. *J. Cell Biol.* 125:381–391.
Nangaku, M., R. Sato-Yoshitake, Y. Okada, Y. Noda, R. Takemura, H. Yamazaki, and N. Hirokawa. 1994. KIF1B, a novel microtubule plus end-directed monomeric motor protein for transport of mitochondria. *Cell.* 79: 1209–1220.
Palmer, R.E., D.S. Sullivan, T. Huffaker, and D. Koshland. 1992. Role of astral microtubules and actin in spindle orientation and migration in the budding yeast, *Saccharomyces cerevisiae. J. Cell Biol.* 119:583–593.
Pearson, W.R., and D.J. Lipman. 1988. Improved tools for biological sequence analysis. *Proc. Natl. Acad. Sci. USA.* 85:2444–2448.
Peterson, J., Y. Zheng, L. Bender, A. Myers, R. Cerione, and A. Bender. 1994. Interactions between the bud emergence proteins Bem1p and Bem2p and the Rho-type GTPases in yeast. *J. Cell Biol.* 127:1395–1406.
Pittenger, M.F., J.A. Kazzaz, and D.M. Helfman. 1994. Functional properties of nonmuscle tropomyosin isoforms. *Curr. Opin. Cell Biol.* 6:96–104.
Pringle, J.R., R.A. Preston, A.E.M. Adams, T. Stearns, D.G. Drubin, B.K. Haarer, and E.W. Jones. 1989. Fluorescence microscopy methods for yeast. *Methods Cell Biol.* 31:357–435.
Pringle, J.R., A.E.M. Adams, D.G. Drubin, and B.K. Haarer. 1991. Immunofluorescence methods for yeast. *Methods Enzymol.* 194:565–602.
Rayment, I., H.M. Holden, M. Whittaker, C.B. Yohn, M. Lorenz, K.C. Holmes, and R.A. Milligan. 1993. Structure of the actin-myosin complex and its implications for muscle contraction. *Science (Wash. DC).* 261:58–65.
Roeder, A.D., and J.M. Shaw. 1996. Vacuole partitioning during meiotic division in yeast. *Genetics.* 144:445–458.
Rose, M.D., and J.R. Broach. 1991. Cloning genes by complemenation in yeast. *Methods Enzymol.* 194:195–230.
Rose, M.D., P. Novick, J.H. Thomas, D. Botstein, and G.R. Fink. 1987. A *Saccharomyces cerevisiae* genomic plasmid bank based on a centromere-containing shuttle vector. *Gene (Amst.).* 60:237–243.
Rothstein, R. 1991. Targeting, disruption, replacement, and allele rescue: integrative DNA transformation in yeast. *Methods Enzymol.* 194:281–301.
Ryan, K.R., and R.E. Jensen. 1995. Protein translocation across mitochondrial membranes: what a long, strange trip it is. *Cell.* 83:517–519.
Schroder, R.R., D.J. Manstein, W. Jahn, H. Holden, I. Rayment, K.C. Holmes, and J.A. Spudich. 1993. Three-dimensional atomic model of F-actin decorated with *Dictyostelium* myosin S1. *Nature (Lond.).* 364:171–174.
Schwarz, E., and W. Neupert. 1994. Mitochondrial protein import: mechanisms, components and energetics. *Biochim. Biophys. Acta.* 1187:270–274.
Sedgwick, S.G., and B.A. Morgan. 1994. Locating, DNA sequencing, and disrupting yeast genes using tagged Tn*1000. Methods Mol. Genet.* 3:131–140.
Shaw, J.M., and W.T. Wickner. 1991. *vac2*: a yeast mutant which distinguishes vacuole segregation from Golgi-to-vacuole protein targeting. *EMBO (Eur. Mol. Biol. Organ.) J.* 10:1741–1748.
Sherman, F., G.R. Fink, and J.B. Hicks. 1986. Methods in Yeast Genetics. Cold Spring Harbor Press, Cold Spring Harbor, NY. 186 pp.
Shortle, D., J.E. Haber, and D. Botstein. 1982. Lethal disruption of the yeast actin gene by integrative DNA transformation. *Science (Wash. DC).* 217:371–373.
Simon, V.R., T.C. Swayne, and L.A. Pon. 1995. Actin-dependent mitochondrial motility in mitotic yeast and cell-free systems: identification of a motor activity on the mitochondrial surface. *J. Cell Biol.* 130:345–354.
Sogo, L.F., and M.P. Yaffe. 1994. Regulation of mitochondrial morphology and inheritance by Mdm10p, a protein of the mitochondrial outer membrane. *J. Cell Biol.* 126:1361–1373.
Stevens, B. 1981. Mitochondrial structure. *In* Molecular Biology of the Yeast *Saccharomyces.* J.M. Strathern, E.W. Jones, and J.R. Broach, editors. Cold Spring Harbor Press, Cold Spring Harbor, NY. 471–504.
Stewart, L.C., and M.P. Yaffe. 1991. A role for unsaturated fatty acids in mitochondrial movement and inheritance. *J. Cell Biol.* 115:1249–1257.
Stromer, M.H., and M. Bendayan. 1990. Immunocytochemical identification of cytoskeletal linkages to smooth muscle cell nuclei and mitochondria. *Cell Motil. Cytoskeleton.* 17:11–18.
Stukey, J.E., V.M. McDonough, and C.E. Martin. 1989. Isolation and characterization of *OLE1*, a gene affecting fatty acid desaturation from *Saccharomyces cerevisiae. J. Biol. Chem.* 264:16537–16544.
Stukey, J.E., V.M. McDonough, and C.E. Martin. 1990. The *OLE1* gene of *Saccharomyces cerevisiae* encodes the Δ9 fatty acid desaturase and can be functionally replaced by the rat stearoyl-CoA desaturase gene. *J. Biol. Chem.* 265:20144–20149.
Summerhayes, I.C., D. Wong, and L.B. Chen. 1983. Effect of microtubules and intermediate filaments on mitochondrial distribution. *J. Cell Sci.* 61:87–105.
Thorsness, P.E. 1992. Structural dynamics of the mitochondrial compartment. *Mutat. Res.* 275:237–241.
Wang, T., and A. Bretscher. 1995. The *rho*-GAP encoded by *BEM2* regulates cytoskeletal structure in budding yeast. *Mol. Biol. Cell.* 6:1011–1024.
Warren, G., and W. Wickner. 1996. Organelle inheritance. *Cell.* 84:395–400.
Welch, M.D., D.A. Holtzman, and D.G. Drubin. 1994. The yeast actin cytoskeleton. *Curr. Opin. Cell Biol.* 6:110–119.
Winston, F., C. Dollard, and S.L. Ricupero-Hovasse. 1995. Construction of a set of convenient *Saccharomyces cerevisiae* strains that are isogenic to S228C. *Yeast.* 11:53–55.
Yaffe, M.P. 1991. Organelle inheritance in the yeast cell cycle. *Trends Cell Biol.* 1:160–163.
Zelenaya-Troitskaya, O., P.S. Perlman, and R.A. Butow. 1995. An enzyme in yeast mitochondria that catalyzes a step in branched-chain amino acid biosynthesis also functions in mitochondrial DNA stability. *EMBO (Eur. Mol. Biol. Organ.) J.* 14:3268–3276.